# Surface smoothing during plasma etching of Si in Cl2

Nobuya Nakazaki, Haruka Matsumoto, Hirotaka Tsuda, Yoshinori Takao, Koji Eriguchi, and Kouichi Ono

Citation: Applied Physics Letters **109**, 204101 (2016); doi: 10.1063/1.4967474
View online: http://dx.doi.org/10.1063/1.4967474
View Table of Contents: http://scitation.aip.org/content/aip/journal/apl/109/20?ver=pdfcov
Published by the AIP Publishing

# Surface smoothing during plasma etching of Si in $Cl_2$

Nobuya Nakazaki,[a] Haruka Matsumoto,[b] Hirotaka Tsuda,[c] Yoshinori Takao,[d] Koji Eriguchi, and Kouichi Ono[e]
*Department of Aeronautics and Astronautics, Graduate School of Engineering, Kyoto University, Kyoto-daigaku Katsura, Nishikyo-ku, Kyoto 615-8540, Japan*

(Received 24 August 2016; accepted 27 October 2016; published online 14 November 2016)

Effects of initial roughness on the evolution of plasma-induced surface roughness have been investigated during Si etching in inductively coupled $Cl_2$ plasmas, as a function of rf bias power or ion incident energy in the range $E_i \approx 20$–500 eV. Experiments showed that smoothing of initially rough surfaces as well as non-roughening of initially planar surfaces can be achieved by plasma etching in the smoothing mode (at high $E_i$) with some threshold for the initial roughness, above which laterally extended crater-like features were observed to evolve during smoothing. Monte Carlo simulations of the surface feature evolution indicated that the smoothing/non-roughening is attributed primarily to reduced effects of the ion scattering or reflection from microscopically roughened feature surfaces on incidence. *Published by AIP Publishing*. [http://dx.doi.org/10.1063/1.4967474]

Atomic- or nanometer-scale roughness on etched feature surfaces has become an important issue to be resolved in the fabrication of nanoscale microelectronic devices, where the roughness formed during plasma etching is often comparable to the critical dimension of the feature and the thickness of the layer being etched and/or the layer underlying.[1–4] In three-dimensional (3D) devices such as fin-type field effect transistors, e.g., the line edge/width roughness formed on fin and gate sidewalls causes a rough channel surface and non-uniform gate length, leading to an increased variability in transistor performance.[5,6] The roughness formed at the feature bottom in gate etch processes is responsible for a recess and damage in substrates and thus also leads to the transistor performance variability.[7] The low degree of surface roughening is also key to fabricating microelectromechanical systems, where the stringent tolerance and topological precision are of most importance.[8–10]

Extensive studies have been made to understand the mechanisms responsible for the formation and evolution of surface roughness during plasma etching of blank (or planar) Si substrates.[1,3,11–26] The mechanisms include the noise (or stochastic roughening),[1,14–17,21] geometrical shadowing,[14,23] surface reemission of etchants,[15–17,19] micromasking by etch inhibitors,[3,20] and ion scattering/channeling.[1,21,24–26] However, the understanding has still not been fully established. We have recently performed experiments of roughness formed during inductively coupled plasma (ICP) etching of Si in $Cl_2$,[24,25] where we found two modes of surface roughening which occur depending on the ion incident energy $E_i$:[25] one is the roughening mode at low $E_i < E_p \approx 200$–300 eV, where the root-mean-square (rms) roughness of etched surfaces increases with increasing $E_i$, exhibiting an almost linear increase with time during etching; the other is the smoothing (or non-roughening) mode at high $E_i > E_p$, where the rms roughness decreases substantially with $E_i$ down to a low level of stochastic roughening (RMS $< 0.5$ nm), exhibiting a quasi-steady behavior soon after only a little increase at the initial stage. A comparison with several plasma diagnostics, Monte Carlo (MC)-based 3D atomic-scale cellular model (ASCeM-3D) simulations for surface feature evolution,[24] and classical molecular dynamics (MD) simulations for etch fundamentals[27] revealed that:[25] the roughening-smoothing transition (at the transition point $E_p$) results primarily from reduced effects of the ion scattering or reflection from microscopically roughened feature surfaces on incidence at increased $E_i$, caused by a change in the predominant ion flux from feed gas ions $Cl_x^+$ to ionized etch products $SiCl_x^+$ owing to the increased etch rates thereat.

In this letter, we report on the evolution of surface roughness of initially rough substrates during ICP $Cl_2$ plasma etching of Si, demonstrating that rough surfaces can be smoothed in the smoothing mode with some threshold for the initial roughness. Such an understanding, under what conditions plasma etching results in surface roughening and/or smoothing and what are the mechanisms concerned, would be of great technological importance. In practice, plasma etching is generally appreciated to result in roughening of surfaces,[1–4] while little systematic/mechanistic work has been concerned with surface smoothing.[11,23] Thomas *et al.*[11] and Martin and Cunge[23] found plasma conditions where etching processes do not generate roughness but smoothen an initially rough surface of Si in $Cl_2$[11,23] and $SF_6$;[23] the latter two authors ascribed the smoothing to the shadowing effects for neutral etchants.

The experimental setup has been detailed in the previous paper;[25] briefly, the ICP discharge was established by 13.56-MHz rf powers of $P_{ICP} = 450$ W, and the wafer stage was rf-biased at 13.56-MHz, being temperature controlled at $T_s = 20\,^{\circ}$C. The rf bias power was varied in the range $P_{rf} = 0$–200 W to vary the ion energy in the range $E_i = V_p - V_{dc} \approx 13$–570 eV, where $V_p$ and $V_{dc}$ are the plasma potential and

[a]Present address: Sony Semiconductor Solutions Corporation, Imaging Device Development Division, Atsugi, Kanagawa 243-0014, Japan.
[b]Present address: Nippon Steel and Sumitomo Metal Corporation, Nagoya Works, Tokai, Aichi 476-8686, Japan.
[c]Present address: Toshiba Corporation Semiconductor and Storage Products Company, Center for Semiconductor Research and Development, Kawasaki, Kanagawa 212-8583, Japan.
[d]Present address: Division of Systems Research, Faculty of Engineering, Yokohama National University, Yokohama, Kanagawa 240-8501, Japan.
[e]Electronic addresses: ono@kuaero.kyoto-u.ac.jp and ono.kouichi.63s@st.kyoto-u.ac.jp

dc self-bias voltage at the wafer stage measured by a Langmuir probe (LP) and a voltage probe, respectively. Pure $Cl_2$ gases were introduced into the ICP chamber at a flow rate $F_0 = 20$ sccm and pressure $P_0 = 20$ mTorr.

Samples for etching were 4-in.-diam blank Si(100) wafers of *n*-type with a resistivity of $\rho_r \approx 10$ and 0.02 Ω cm, which were cleaned through HF acid dipping followed by deionized water rinsing, defining a reference planar surface with an rms roughness RMS ≈ 0.15 nm. Initially rough surfaces of Si were then generated through a roughening step by plasma etching in $Cl_2$ at $P_{rf} = 30$ W (or $E_i \approx 120$ eV).[25] The roughening time was varied in the range $t_{rough} = 0$–5 min, to prepare sample substrates with different initial surface roughness in the range $RMS_0 \approx 0.15$–6.6 nm,[28] and the following main etch time was varied in the range $t_{etch} = 0$–5 min. The etched and unetched sample surfaces were examined by atomic force microscopy (AFM) to measure the rms surface roughness and to analyze the power spectral density (PSD) of surface features, where the AFM images were acquired in tapping mode on a scan area of $1 \times 1\ \mu m^2$ with the resolution of $256 \times 256$ pixels. The surface images were also taken by scanning electron microscopy (SEM). Moreover, the etched depth and thus the etch rate was measured by using stylus profilometry, where thermal $SiO_2$ films were also etched to measure the etch selectivity. The results for initially planar surfaces of $RMS_0 \approx 0.15$ nm (partly shown below) have been detailed previously,[25] along with plasma conditions of the discharge diagnosed by LP, optical emission spectroscopy, infrared absorption spectroscopy, and quadrupole mass spectrometry.

Figure 1 shows the etch rate and rms surface roughness of Si as a function of ion energy in the range $E_i \approx 22$–520 eV, obtained in ICP $Cl_2$ plasma etching ($t_{etch} = 2$ min) for different $RMS_0 \approx 0.15$–6.6 nm. Also shown is the $SiO_2$ etch rate as a function of $E_i$. The results indicate that as $E_i$ is increased, the Si and $SiO_2$ etch rates increase, and the selectivity of Si over $SiO_2$ decreases, where the Si etch rate is almost independent of $RMS_0$, implying that the surface reaction kinetics are not affected significantly by the surface roughness; on the other hand, the rms roughness of etched Si surfaces for any $RMS_0$ increases (roughening mode), peaks at around $E_i = E_p \approx 200$–300 eV (depending slightly on $RMS_0$), and then decreases (smoothing mode). It should be noted that at $E_i > E_p$, the rms surface roughness decreases substantially down to the low level of RMS < 0.5 nm for $RMS_0 < 2.2$ nm, while it remains higher than the initial $RMS_0$ for $RMS_0 > 3.7$ nm, indicating that initially rough surfaces are smoothed by plasma etching in the smoothing mode with some threshold $RMS_{0th} \approx 3$ nm.

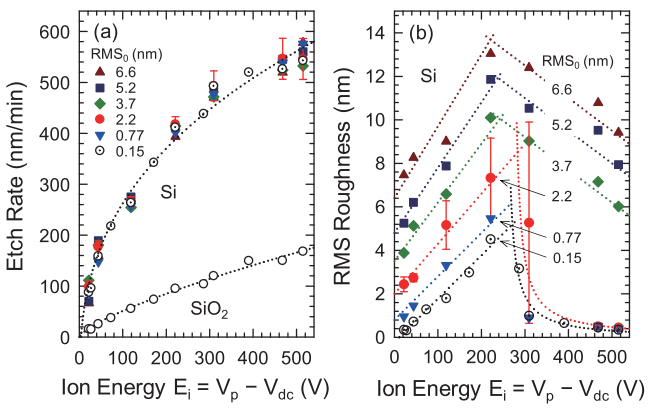


FIG. 1. (a) Etch rate and (b) rms surface roughness of Si as a function of ion incident energy in the range $E_i \approx 22$–520 eV, obtained in ICP $Cl_2$ plasma etching ($t_{etch} = 2$ min) for different initial surface roughness $RMS_0 \approx 0.15$–6.6 nm. The error bars (shown typically for $RMS_0 \approx 2.2$ nm) represent the variation in the raw data for more than ten etching experiments using Si wafers with different resistivities; the data on the roughness at $E_i \approx 220$ and 310 eV have significantly large error bars, corresponding to the roughening-smoothing transition regime. Also shown in (a) is the $SiO_2$ etch rate as a function of $E_i$. The dotted lines are for guiding the eyes only.

Figure 2 shows the rms surface roughness of Si as a function of time in the range $t_{etch} = 0$–5 min, obtained in ICP $Cl_2$ plasma etching for two different $RMS_0 \approx 2.2$ and 6.6 nm at $E_i \approx 22$–520 eV. The results indicate that for weakly roughened $RMS_0 \approx 2.2$ nm (<$RMS_{0th}$), the rms roughness at $E_i < E_p$ (roughening mode) increases almost linearly with time during etching, where the higher the $E_i$, the larger is the increase in roughness; in contrast, at $E_i > E_p$ (smoothing mode), the roughness decreases down to the low level of RMS < 0.5 nm soon after the start of etching ($t < 1$–2 min). On the other hand, for highly roughened $RMS_0 \approx 6.6$ nm (>$RMS_{0th}$), the rms roughness at $E_i < E_p$ increases almost linearly with time, similar to the tendency for $RMS_0 \approx 2.2$ nm; in contrast, at $E_i > E_p$, the roughness initially increases for a while ($t < 1$–2 min) and then decreases, which appears to be different partly from the behavior of $RMS_0 \approx 2.2$ nm. The Si etch rate concerned was observed to reach a quasi-steady state soon after the start of etching, implying that the roughness evolution does not follow that of the etch rate as in Fig. 1.

Figure 3 shows typical SEM images of the time evolution of Si surfaces etched in ICP $Cl_2$ plasmas ($t_{etch} = 0$–5 min) for two different $RMS_0 \approx 2.2$ and 6.6 nm at $E_i \approx 120$ and 470 eV. These SEM images are consistent with the data of the rms surface roughness in Figs. 1(b) and 2: at $E_i \approx 120$ eV (roughening mode), the surface roughness continues to evolve with time during etching for any $RMS_0$; in contrast, at $E_i \approx 470$ eV (smoothing mode), the roughness for $RMS_0 \approx 2.2$ nm (<$RMS_{0th}$) decreases down to a low level soon after the start

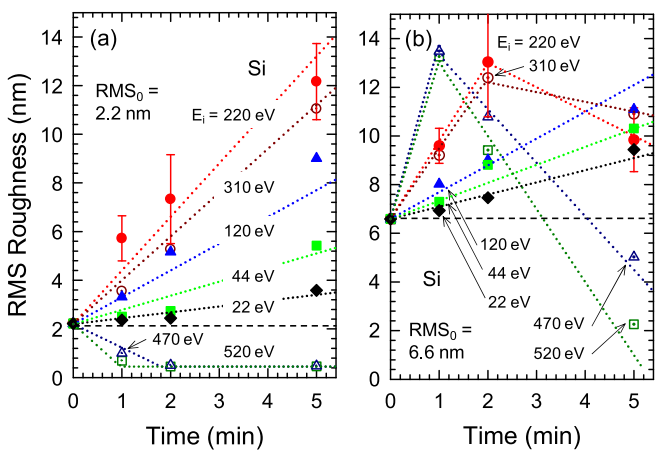


FIG. 2. RMS surface roughness of Si as a function of etching time in the range $t_{etch} = 0$–5 min, obtained in ICP $Cl_2$ plasma etching for two different initial surface roughness $RMS_0 \approx$ (a) 2.2 and (b) 6.6 nm at ion incident energies of $E_i \approx 22$–520 eV. The rms roughness at $t_{etch} = 0$ is the initial $RMS_0$, and the error bars shown have the same properties as in Fig. 1. The dotted lines are for guiding the eyes only.

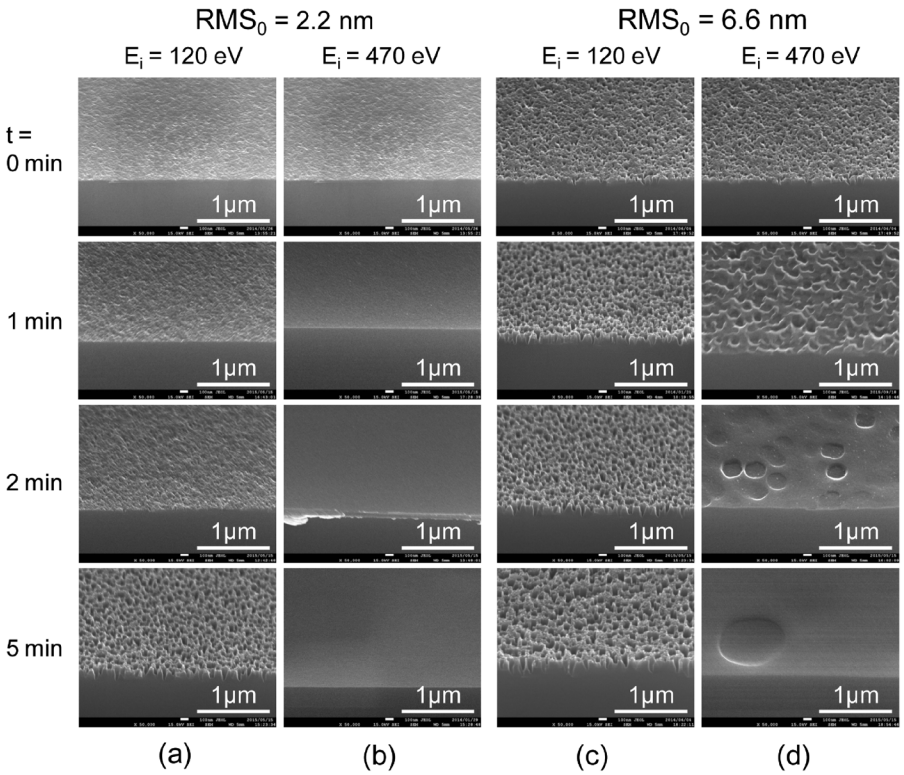


FIG. 3. Typical SEM images of the time evolution of Si surfaces etched in ICP $Cl_2$ plasmas ($t_{etch} = 0$–5 min) for two different initial surface roughness $RMS_0 \approx$ (a), (b) 2.2 and (c), (d) 6.6 nm at ion incident energies of $E_i \approx 120$ and 470 eV. The image at $t_{etch} = 0$ is that of the initial $RMS_0$, and these SEM images were consistent visually with the corresponding AFM images (not shown).

of etching, while that for $RMS_0 \approx 6.6$ nm ($>RMS_{0th}$) initially increases for a while ($t < 1$ min) and then decreases. It should be noted that for $RMS_0 \approx 6.6$ nm at $E_i \approx 470$ eV, the SEM images exhibit shallow crater-like features during smoothing ($t > 2$ min), whose lateral extent increases significantly with time without a significant change in vertical depth; at much later times ($t > 5$ min), they were found to eventually fade away from the SEM scan area with smooth surfaces remaining thereafter.

Figure 4 shows the time evolution of the angularly averaged PSD distribution $P(k)$ of Si surfaces etched in ICP $Cl_2$ plasmas ($t_{etch} = 0$–5 min) for two different $RMS_0 \approx 2.2$ and 6.6 nm at $E_i \approx 120$ and 470 eV. Also shown for reference are the $P(k)$ curve at $t_{etch} = 0$ and that at $t_{etch} = 5$ min ($E_i \approx 470$ eV) for initially planar $RMS_0 \approx 0.15$ nm.[25] The roughness parameters of interest are:[12,22–25] the plateau height value $w_0$ at low spatial frequency $k$ related to the vertical height/depth of roughened surface features [$P(k) \approx w_0$ at $k < k_0$], and the correlation length $\xi_0$ that defines the lateral (or spatial) extent of the roughness ($\xi_0 = 1/k_0 \approx 50$, 140, and 250 nm at $t = 0$ for $RMS_0 \approx 0.15$, 2.2, and 6.6 nm, respectively); the $P(k)$ tail at high $k$ gives a fractal nature of the roughness [$P(k) \approx K/k^{\eta}$ at $k > k_0$], where $K$ is the spectral strength, and the exponent $\eta$ is linked to the fractal dimension.

The PSD analyses indicate that at $E_i \approx 120$ eV (roughening mode), the $P(k)$ magnitudes at low and high $k$ increase ($w_0$ and $K$ increase along with $\xi_0$) during etching for any $RMS_0$, without a significant change in $\eta \approx 3$ of the $P(k)$ tail, corresponding to the increase in both vertical and lateral roughness. In contrast, at $E_i \approx 470$ eV (smoothing mode), the $P(k)$ magnitude for $RMS_0 \approx 2.2$ nm ($< RMS_{0th}$) decreases at low and high $k$ ($w_0$ and $K$ decrease along with $\xi_0$), significantly at the initial stage ($t < 1$ min) and then gradually thereafter, without a significant change in $\eta$. It should be noted that the $P(k)$ curve at later times ($t > 2$ min) for $RMS_0 \approx 2.2$ nm tends to be similar to that of $RMS_0 \approx 0.15$ nm, corresponding to the low level of stochastic roughening in the smoothing mode.

It should be further noted that at $E_i \approx 470$ eV, the $P(k)$ evolution for $RMS_0 \approx 6.6$ nm ($>RMS_{0th}$) appears to be partly different from that of $RMS_0 \approx 2.2$ nm, as in Figs. 2 and 3: it exhibits the behavior of surface roughening at the initial stage ($t < 1$ min). Then, the $P(k)$ exhibits that of surface smoothing thereafter; concretely, in Fig. 4(d), the $P(k)$ magnitudes at low and high $k$ decrease with time towards the low level of stochastic roughening without a significant change in $\eta$ of the $P(k)$ tail. However, during smoothing ($t > 2$ min), the $P(k)$ curve for $RMS_0 \approx 6.6$ nm tends to have two separate regimes of the roughness evolution[29,30] at low and high $k$; the low-frequency (or long) correlation length is increased with time as $\xi_0 = 1/k_0 \approx 300$, 400, and 1000 nm at $t = 1$, 2, and 5 min, respectively. In these situations, lower-frequency roughness components (at $k < k_0$) tend to remain on the surface, which would be smoothed in a much longer time scale; in effect, the $w_0$ and $\xi_0$ at low $k$ tend to be unclear at much later times ($t > 5$ min), because $\xi_0$ or the lateral extent of the low-frequency roughness [related to crater-like features as in SEM images of Fig. 3(d)] increases with time to exceed the limit length $W_A = 1$ $\mu$m or its reciprocal $k = 0.001$ nm$^{-1}$ of the AFM scan area.

Figure 5 shows the rms surface roughness of Si as a function of time in the range $0 \le t \le 40$ s for different $RMS_0 = 0.1$–6 nm in the roughening and smoothing modes, obtained through ASCeM-3D simulations for Si etching in $Cl_2$ plasmas assuming similar conditions to those in experiments.[25] Inset are typical surface features at different times during smoothing simulated for $RMS_0 = 4$ nm. The ASCeM-3D is our original 3D MC-based simulation model for

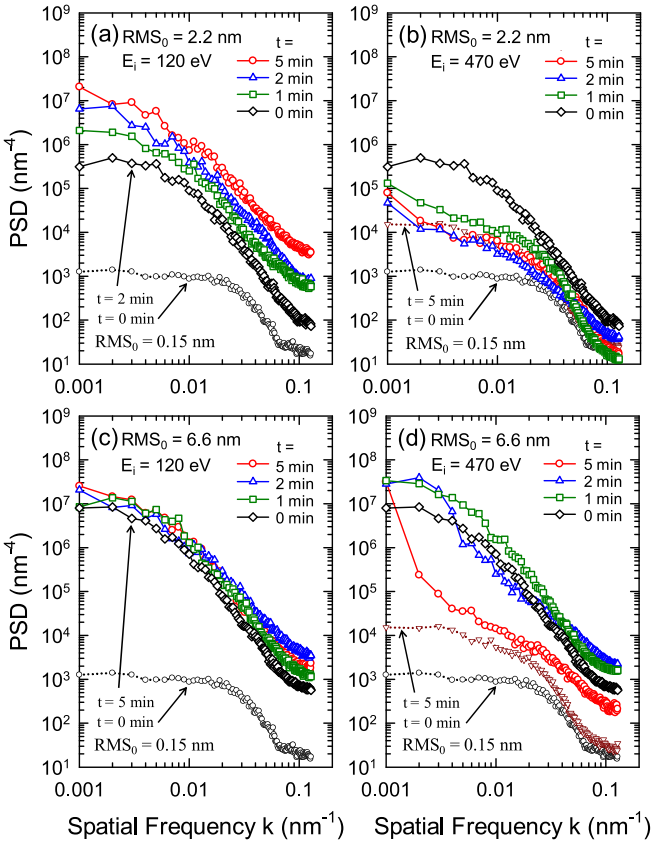


FIG. 4. Time evolution of the angularly averaged PSD distribution $P(k)$ of Si surfaces etched in ICP $Cl_2$ plasmas ($t_{etch} = 0$–5 min) for two different initial surface roughness $RMS_0 \approx$ (a), (b) 2.2 and (c), (d) 6.6 nm at ion incident energies of $E_i \approx 120$ and 470 eV. The PSD distribution at $t_{etch} = 0$ is that of the initial $RMS_0$. Also shown for reference are the $P(k)$ curve at $t_{etch} = 0$ and that at $t_{etch} = 5$ min ($E_i \approx 470$ eV) for initially planar $RMS_0 \approx 0.15$ nm (Ref. 25). The spatial frequency ranges from $k = 0.001$ to $0.128\ nm^{-1}$, corresponding to the side length $W_A = 1\ \mu m$ of the AFM scan area with the resolution of 256 pixels. Note that initially rough surfaces of $RMS_0 \approx 2.2$ and 6.6 nm were generated from initially planar surfaces of $RMS_0 \approx 0.15$ nm through a roughening step by plasma etching or plasma exposure in $Cl_2$ at $E_i \approx 120$ eV with $t_{rough}$ (or $t_{etch}$) = 2 and 5 min, respectively (Ref. 28).

plasma-surface interactions and the feature profile evolution during $Cl_2$-based plasma etching of Si, which has been detailed previously.[24] Calculations were made for square substrates $W = 50$ nm on a side, with an incoming ion ($Cl^+$) flux $\Gamma_i^0 = 1.0 \times 10^{16}\ cm^{-2} s^{-1}$, neutral reactant (Cl)-to-ion flux ratio $\Gamma_n^0/\Gamma_i^0 = 100$, and impurity oxygen (O)-to-ion flux ratio $\Gamma_o^0/\Gamma_i^0 = 0.002$, where a small amount of O (hard inhibitor) was assumed to originate from the dielectric rf window of the ICP reactor;[25] the ion and neutral temperatures were assumed to be $k_B T_i = 0.5$ eV and $T_g = 500$ K, respectively, along with a surface temperature $T_s = 320$ K of substrates. Initial substrate surfaces were prepared from a flat model surface (RMS = 0) through ASCeM-3D roughening simulation as in experiments. In these calculations, the roughening mode was simulated with $E_i = 100$ eV and an ion reflection coefficient $r_i = 1$ (assuming the predominant ion fluxes of reactive $Cl_2^+$ and $SiCl_3^+$), while the smoothing mode was with $E_i = 500$ eV and a reduced $r_i = 0.8$ (assuming those of depositive $SiCl^+$),[25,31] based on the results of plasma diagnostics[25] and MD simulations.[27,32]

A comparison with experiments indicates that the ASCeM-3D reproduces an increase in the rms surface roughness of Si with time in the roughening mode; the

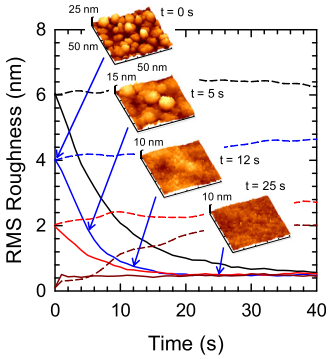


FIG. 5. RMS surface roughness of Si as a function of etching time in the range $0 \le t \le 40$ s for different initial surface roughness $RMS_0 = 0.1$, 2, 4, and 6 nm in the smoothing mode (solid lines), together with that in the roughening mode (broken lines), obtained through ASCeM-3D simulations for Si etching in $Cl_2$ plasmas with normal ion incidence ($\theta_i = 0°$) assuming similar conditions to those in experiments. The rms roughness at $t = 0$ is the initial $RMS_0$. These are the typical runs of the calculation (including effects of a small amount of impurity oxygen), where the roughening mode was simulated with $E_i = 100$ eV and an ion reflection coefficient $r_i = 1$, while the smoothing mode was with $E_i = 500$ eV and a reduced $r_i = 0.8$. Inset are typical surface features at different times during smoothing simulated for $RMS_0 = 4$ nm.

ASCeM-3D also reproduces well a smooth surface at the low level of stochastic roughening (RMS < 0.5 nm) for $RMS_0 = 0.1$ nm and a decrease in rms roughness down to the similar low level for $RMS_0 = 2$–6 nm in the smoothing mode. Thus, the smoothing/non-roughening of surfaces during etching is attributed primarily to reduced effects of the ion reflection from microscopically roughened feature surfaces on incidence in the smoothing mode. In addition, the ASCeM-3D etch rate of Si exhibited a quasi-steady value soon after the start of etching,[24,25] which was consistent with that in experiments [Fig. 1(a)].

However, for $RMS_0 = 4$–6 nm ($>RMS_{0th}$) in the smoothing mode, the ASCeM-3D does not reproduce an initial increase in rms roughness and the following evolution of laterally extended crater-like features during smoothing visible in experiments. The crater-like features seem to originate from the initial local defects formed, e.g., in preparing initially rough surfaces through plasma exposure; in effect, such lower-frequency or longer-wavelength features of the roughness would not be smoothed before a longer period, because effects of the ion reflection as well as neutral shadowing are assumed to be smaller for lower aspect-ratio features.[33] Moreover, the initial increase in roughness may be attributable to transient plasma conditions in the smoothing mode; in practice, the plasma is considered to change from $Cl_x^+$-rich to $SiCl_x^+$-rich regimes in a while after the start of etching, which would affect more largely the roughness evolution for higher $RMS_0$. Further investigations are needed to identify all the mechanisms concerned, including separate sample preparation procedures for different $RMS_0$, e.g., by using wet chemical process.[34]

In conclusion, we have demonstrated that smoothing of initially rough surfaces as well as non-roughening of initially planar surfaces of Si can be achieved by $Cl_2$ plasma etching in the smoothing mode (at $E_i > E_p \approx 200$–300 eV) with some threshold ($RMS_{0th} \approx 3$ nm) for the initial roughness. The MC-based ASCeM-3D simulations reproduced well the

smoothing/non-roughening of surfaces with reduced effects of the ion scattering or reflection from microscopically roughened feature surfaces on incidence. These understandings may not be inconsistent with the atomic layer etching of Si,[4,35,36] where low-energy (∼50 eV) $Ar^+$ ion impacts[37] on chlorinated surfaces do little roughening on their own; in our situations, the lower the $E_i$, the smoother will be the surfaces etched, if the smoothing mode is achieved at lower $E_i$, as the ASCeM-3D indicated.[31]

This work was supported by Grants-in-Aid for Scientific Research (21110008 and 15H03582) from MEXT and JSPS, Japan. One of the authors (N.N.) was supported by Research Fellowships from the JSPS for Young Scientists. The authors would also like to thank T. Hatsuse (presently at Nippon Steel and Sumitomo Metal Corporation) for assistance with ASCeM-3D simulations.

[1]W. Guo and H. H. Sawin, J. Phys. D: Appl. Phys. **42**, 194014 (2009).
[2]G. S. Oehrlein, R. J. Phaneuf, and D. B. Graves, J. Vac. Sci. Technol., A **29**, 010801 (2011).
[3]E. Gogolides, V. Constantoudis, G. Kokkoris, D. Kontziampasis, K. Tsougeni, G. Boulousis, M. Vlachopoulou, and A. Tserepi, J. Phys. D: Appl. Phys. **44**, 174021 (2011).
[4]K. J. Kanarik, T. Lill, E. A. Hudson, S. Sriraman, S. Tan, J. Marks, V. Vahedi, and R. A. Gottscho, J. Vac. Sci. Technol., A **33**, 020802 (2015).
[5]K. Patel, T.-J. King Liu, and C. J. Spanos, IEEE Trans. Electron Devices **56**, 3055 (2009).
[6]E. Altamirano-Sánchez, V. Paraschiv, M. Demand, and W. Boullart, Microelectron. Eng. **88**, 2871 (2011).
[7]K. Eriguchi, Y. Takao, and K. Ono, J. Vac. Sci. Technol., A **29**, 041303 (2011).
[8]K. S. Chen, A. Ayon, and S. M. Spearing, J. Am. Ceram. Soc. **83**, 1476 (2000).
[9]N. Tayebi and A. A. Polycarpou, J. Appl. Phys. **98**, 073528 (2005).
[10]D. F. Jaramillo-Cabanzo, G. A. Willing, and M. K. Sunkara, ECS Solid State Lett. **4**, P80 (2015).
[11]D. J. Thomas, P. Southworth, M. C. Flowers, and R. Greef, J. Vac. Sci. Technol., B **7**, 1325 (1989).
[12]R. Pétri, P. Brault, O. Vatel, D. Henry, E. André, P. Dumas, and F. Salvan, J. Appl. Phys. **75**, 7498 (1994).
[13]K.-T. Sung and S. W. Pang, Jpn. J. Appl. Phys., Part 1 **33**, 7112 (1994).
[14]P. Brault, P. Dumas, and F. Salvan, J. Phys. Condens. Matter **10**, L27 (1998).
[15]Y.-P. Zhao, J. T. Drotar, G.-C. Wang, and T.-M. Lu, Phys. Rev. Lett. **82**, 4882 (1999).
[16]J. T. Drotar, Y.-P. Zhao, T.-M. Lu, and G.-C. Wang, Phys. Rev. B **61**, 3012 (2000).
[17]J. T. Drotar, Y.-P. Zhao, T.-M. Lu, and G.-C. Wang, Phys. Rev. B **62**, 2118 (2000).
[18]E. Gogolides, C. Boukouras, G. Kokkoris, O. Brani, A. Tserepi, and V. Constantoudis, Microelectron. Eng. **73–74**, 312 (2004).
[19]E. Zakka, V. Constantoudis, and E. Gogolides, IEEE Trans. Plasma Sci. **35**, 1359 (2007).
[20]G. Kokkoris, V. Constantoudis, P. Angelikopoulos, G. Boulousis, and E. Gogolides, Phys. Rev. B **76**, 193405 (2007).
[21]Y. Yin and H. H. Sawin, J. Vac. Sci. Technol., A **26**, 151 (2008).
[22]W. S. Hwang, B.-J. Cho, D. S. H. Chan, S. W. Lee, and W. J. Yoo, J. Electrochem. Soc. **155**, H6 (2008).
[23]M. Martin and G. Cunge, J. Vac. Sci. Technol., B **26**, 1281 (2008).
[24]H. Tsuda, N. Nakazaki, Y. Takao, K. Eriguchi, and K. Ono, J. Vac. Sci. Technol., B **32**, 031212 (2014), and references therein.
[25]N. Nakazaki, H. Tsuda, Y. Takao, K. Eriguchi, and K. Ono, J. Appl. Phys. **116**, 223302 (2014), and references therein.
[26]O. Mourey, C. Petit-Etienne, G. Cunge, M. Darnon, E. Despiau-Pujo, P. Brichon, E. Lattu-Romain, M. Pons, and O. Joubert, J. Vac. Sci. Technol., A **34**, 041306 (2016).
[27]N. Nakazaki, Y. Takao, K. Eriguchi, and K. Ono, Jpn. J. Appl. Phys. **53**, 056201 (2014); J. Appl. Phys. **118**, 233304 (2015).
[28]Surfaces of different initial roughness $RMS_0 \approx 0.15$, 0.77, 2.2, 3.7, 5.2, and 6.6 nm were prepared from wet-cleaned planar Si substrates of RMS ≈ 0.15 nm through a roughening step with $t_{rough}$ (or $t_{etch}$) = 0, 1, 2, 3, 4, and 5 min, respectively.
[29]A. E. Lita and J. E. Sanchez, Jr., J. Appl. Phys. **85**, 876 (1999).
[30]D. B. Fenner, J. Appl. Phys. **95**, 5408 (2004).
[31]T. Hatsuse, N. Nakazaki, H. Tsuda, Y. Takao, K. Eriguchi, and K. Ono, "Origin of plasma-induced surface roughening and ripple formation during plasma etching of silicon: A Monte Carlo study," Jpn. J. Appl. Phys. (unpublished).
[32]N. Nakazaki, Y. Takao, K. Eriguchi, and K. Ono, "Molecular dynamics simulations of oblique incidence of silicon chloride ions during Si etching in Cl-based plasmas," Jpn. J. Appl. Phys. (unpublished).
[33]K. Ono, H. Ohta, and K. Eriguchi, Thin Solid Films **518**, 3461 (2010).
[34]P. Karmakar, S. A. Mollick, D. Ghose, and A. Chakrabarti, Appl. Phys. Lett. **93**, 103102 (2008).
[35]H. Sakaue, S. Iseda, K. Asami, J. Yamamoto, M. Hirose, and Y. Horiike, Jpn. J. Appl. Phys., Part 1 **29**, 2648 (1990).
[36]S. D. Athavale and D. J. Economou, J. Vac. Sci. Technol., A **13**, 966 (1995).
[37]F. Ludwig, Jr., C. R. Eddy, Jr., O. Malis, and R. L. Headrick, Appl. Phys. Lett. **81**, 2770 (2002).